SafeWind

Collaborative project funded by the European Commission under the 7th Framework Program, Theme 2007-2.3.2: Energy

"Multi-scale data assimilation, advanced wind modelling & forecasting with emphasis to extreme weather situations for a safe large-scale wind power integration"

Grant Agreement N°: 213740

Deliverable Dc-2.3

"Results of the measurement campaign in complex terrain - Assessment"

DOCUMENT TYPE	Deliverable
DOCUMENT NAME:	swind_deliverable_Dp-2.3_assess_v1.3_Final
VERSION:	V1.3
DATE:	2012.06.21
CLASSIFICATION:	R1: General public
STATUS:	Final

Abstract: This Deliverable of SafeWind project presents an assessment of the lidar and sodar measurements made at the Alaiz complex terrain site. It is found that the remote sensing instruments are affected by the flow inhomogeneity due to the complex terrain, with an error of up to 10%, according to the wind direction. The terrain induced error from the different instruments appears to be of the same order of magnitude. For the continuous wave lidar, measurement errors due to fog and mist are seen to be even more significant than the errors due to the complex terrain.

AUTHORS[1], REVIEWERS				
MAIN AUTHOR/EDITOR:	Fernando Borbon			
AFFILIATION:	CENER			
ADDRESS:	Pol. Rocaforte, Parcelas G2-H1. 31400 Sangüesa, Spain			
TEL.:	+34 948 87 17 45			
EMAIL:	fborbon@cener.com			
FURTHER AUTHORS:	Eric Dupont, Yannick Lefranc			
PEER REVIEWERS:	M. Courtney, R.Girard			
REVIEW APPROVAL:	Approved :		Rejected (improve as indicated below) :	
SUGGESTED IMPROVEMENTS:	*For a long list of remarks make reference to another document*			

VERSION HISTORY			
VERSION[2]:	DATE:	COMMENTS, CHANGES, STATUS:	PERSON(S):

STATUS, CONFIDENTIALITY, ACCESSIBILITY									
STATUS:				CONFIDENTIALITY:				ACCESSIBILITY:	
S0	Approved/Released	**X**		**R0**	General public	**X**		Private web site	
S1	Reviewed			**R1**	Restricted to project members			Public web site	**X**
S2	Pending for review			**R2**	Restricted to European Commission			Paper copy	
S3	Draft for comments			**R3**	Restricted to WP members + PL				
S4	Under preparation			**R4**	Restricted to Task members +WPL+PL				

PL: *Project leader* **WPL:** *Work package leader* **TL:** *Task leader*

[1] **The authors of this document are solely responsible for its content, which does not represent the opinion of the European Community and the European Community is not responsible for any use that might be made of data appearing therein.**

[2] **VERSION NAMING : V0.x** draft before peer-review approval, **V1.0** at the approval, **V1.x** minor revisions, **V2.0** major revision

Contents

1. Experimental set up in complex terrain conditions

A measurement campaign was carried out in complex terrain conditions at CENER's Alaiz test site. The test site includes a total of six met masts of 120 m height, each instrumented identically with cup anemometers, propeller anemometer and wind vanes at four different heights (78, 90, 102 and 118 m) plus an additional anemometer at 40 m. These conditions make the Alaiz test site a very valuable facility for scientific research. In addition, a total of six positions are available for testing multi-megawatt wind turbine prototypes at a complex terrain environment for both commercial and scientific purposes.

The two lidars were installed approximately 20 m west from mast MP5 (see Figure 1-2 d)). A detailed diagram of the met mast instrumentation is presented in Figure 1-1. For each measurement height there are two booms separated approximately 2 m. The higher boom is supporting the reference cup anemometer (east) and the wind vane (west). In the lower boom there is a control cup anemometer (east) and a vertical anemometer (west). Additionally, humidity and temperature sensors are installed at three different heights: 113 m, 97.5 m and 81 m. A rain detector is installed at 5 m and an atmospheric pressure sensor is installed at 1.5 m height.

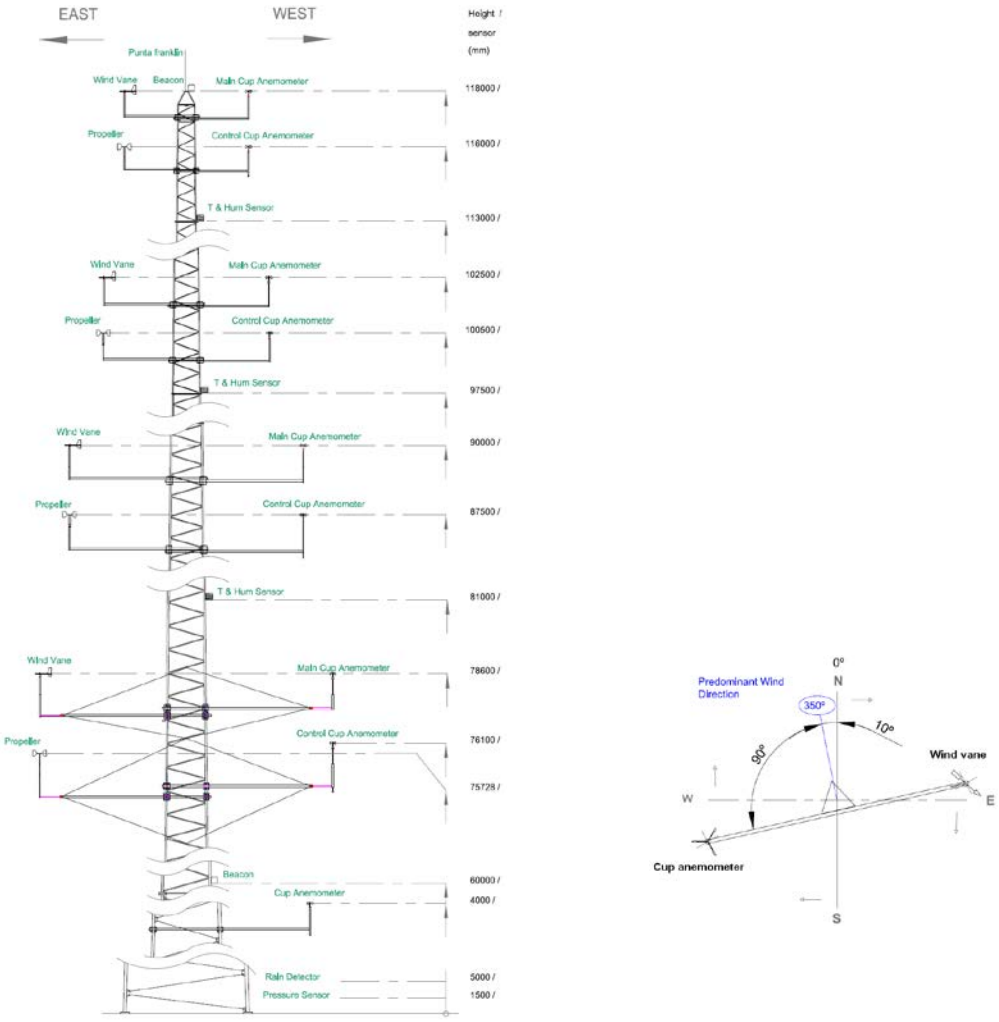

a) Sensor location at several heights at MP5 met mast. b) Met mast alignment.

Figure 1-1. Met mast instrumentation at Alaiz test site.

For the equipment used by CENER, Gómez (2011) indicates that the pressure, temperature and humidity sensors, the propellers, the data acquisition system and the power transducers have been calibrated by laboratories accredited by the UNE-EN ISO/IEC 17025 standard. Additionally, cup anemometers have been calibrated by a laboratory accredited by MEASNET. Furthermore, the equipment installation for the Alaiz met masts has been done following the recommendations given in the IEC 61400-12-1 – Part 12-1 standard.

The test site were the met mast and the lidars are installed, is located on the top of a mountain of approximately 500 m height above the flat surroundings, as seen in Figure 1-2 a). At the mast and lidars' location, the mountain has an almost uniform slope facing north which extends nearly parallel to the west-east direction. Following in north

direction, there is a plateau extending for approximately 15 km as seen in Figure 1-2 b). On the other side, the adjacent mountainous structure follows a south-east direction. In Figure 1-2 c) the altitude at the Alaiz ridge is shown using a contour map. Notice that the test site is located at the highest elevation. Zooming into the test site, the met mast positions are indicated in Figure 1-2 d). The lidars have been installed next to the MP5 met mast.

a) Perspective view of the Alaiz ridge and northern plateau.

b) Alaiz ridge and surroundings orography.

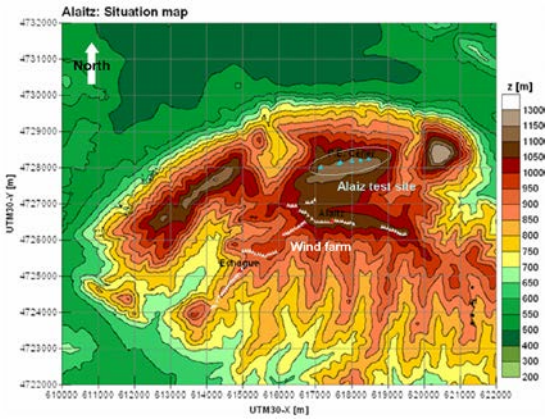

c) Contour map indicating altitude. The position of the Alaiz test site is indicated as well as the sitting of the turbines from a neighbor wind farm. At the lidars' location, the height is 1122 m.

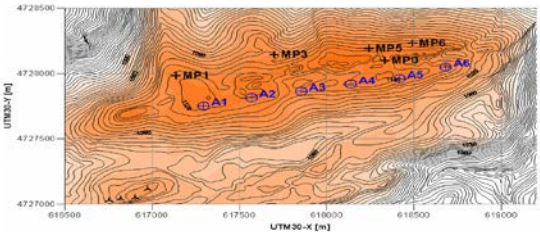

d) Met mast locations at Alaiz test site (MP's) and locations for wind turbine prototypes (A's). The lidars have been installed next to the MP5 mast.

Figure 1-2. Alaiz terrain conditions and met mast positioning.

The two lidars are installed closely to the MP5 met mast as can be seen in Figure 1-3 a). Since the Windcube lidar triggers the laser beam at four defined directions, it is possible to place it close to the met mast structure being careful that none of the beam directions is obstructed by the mast structure. On the other hand, the ZephIR lidar senses the radial velocities at 50 different angles and it is more difficult to avoid completely that some

beam positions will hit the tower structure. Therefore, in order to reduce the number of hitting beams, a larger distance from the met mast is necessary, in this case approximately 15 m. A general view of the test site including all the other met masts is shown in Figure 1-3 b).

a) MP5 met mast and lidars' positioning.

b) General view of the Alaiz test site including the 6 available met masts.

Figure 1-3. Sensing equipment location at Alaiz test site.

The precise location of the lidars in several coordinate systems is given in Table 2.1-1.

Table 2.1-1. Lidars' location at Alaiz test site.

Coordinate system	Value
Geographic	42°41'49.6"N 001°33'23.2"W (42.69711 -1.55643)
UTM/UPS	30N 618240 4728190
MGRS	30TXN1824028190

The MP5 mast is located at the northern side of the test site, precisely at the edge of the mountain. Correspondingly, the lidars were programmed to sense the wind velocity at the four different heights coinciding with those from the met mast instrumentation. All the signal records are saved in a database, thus facilitating the later access and processing of information.

2. Result analysis

2.1 Introduction

The complex terrain measurement campaign extended from October 2010 to June 2011. The analysis of the environmental and orography conditions and their effect on the lidar uncertainty are studied, with special attention paid to the effects of non-uniform wind flow, which has been accredited to play a major role on lidar uncertainty.

Data filtering criteria applied includes: screening of measurements when temperatures were below 2ºC and wind speeds below 4 ms^{-1}. Similarly, other instrument-specific filtering criteria have been applied to ensure the quality of lidar data, such as the minimum values of points in fit and packets in average of the ZephIR, and the availability value (selected to equal 100%) of the Windcube. Similar filtering criteria are found in Gottschall (2010).

Other environmental factors that may affect lidar performance such as rain and fog have been filtered out as well. In particular, fog (i.e. cloud below lidar measurement heights) affects each lidar device in a different way: it results in a lack of measurement in the case of a pulsed lidar (Windcube), and in a wind speed measurement with large negative error in the case of a continuous-wave (CW) lidar (ZephIR). The latter error is of a magnitude considerably greater than the magnitude of the terrain-induced errors, which is the subject of this study. Although fog has been discarded in this study in order to focus on terrain effects, it has been identified as the major source of (CW) lidar error in the complex terrain campaign.

2.2 Wind resource characterization

1.1.1 Wind speed frequency distribution

The wind speed distribution histogram shown in Figure 2-1 corresponds to the nearly 9 months of data for the complex terrain campaign. In this and following figures, the title information indicates the measurement height (H), the wind direction bin (or wind sector) center (B.C.), the wind direction bin width (B.W.), the condition if lidar filters were applied (F) and the number of records (n) that have been plotted after applying quality filters, if the case. The wind speed distribution shows the predominant wind speed is around 8 ms^{-1}. Notice also that the lower and higher wind speeds are evenly distributed along all the wind directions. The maximum wind speed registered during this period is around 23 ms^{-1}.

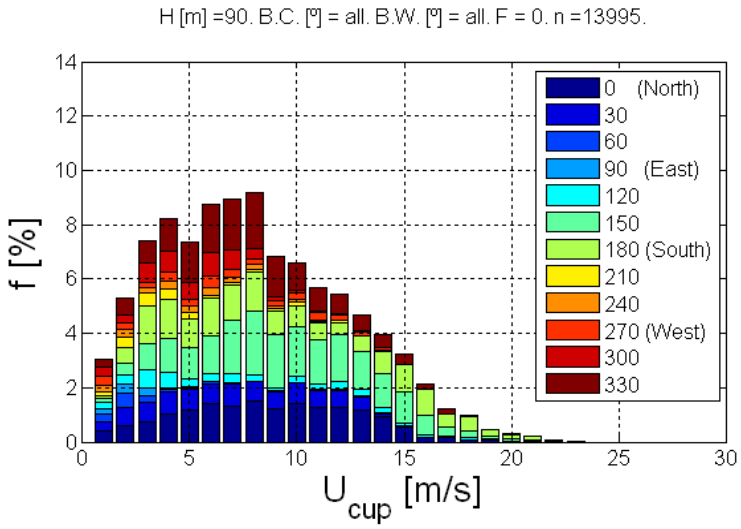

Figure 2-1. Wind speed frequency distribution at 90 m height. Wind direction contributions indicated by different colors.

The wind direction frequency distribution is a relevant feature to characterize the wind conditions at each test site. The lidar error due to complex terrain conditions depends on the terrain properties at each direction and the interaction of these properties with the wind flow. Therefore, a description of the wind direction frequency can help to identify how affected the wind flow is at a specific site when the surrounding terrain orography and the location of large obstacles are known. Moreover, it is possible to assess how statistically representative the wind coming from a specific direction sector is compared to the other directions. This knowledge can be used to refine the data filtering criteria as presented in the following section.

1.1.2 Wind direction frequency distribution

The wind direction frequency distribution is presented in Figure 2-2. The complex terrain site has a wind direction distribution oriented mainly in the north-south axis, coinciding with the steepest slopes. Nearly all the wind is either from the north-west and north or from the south-east and south.

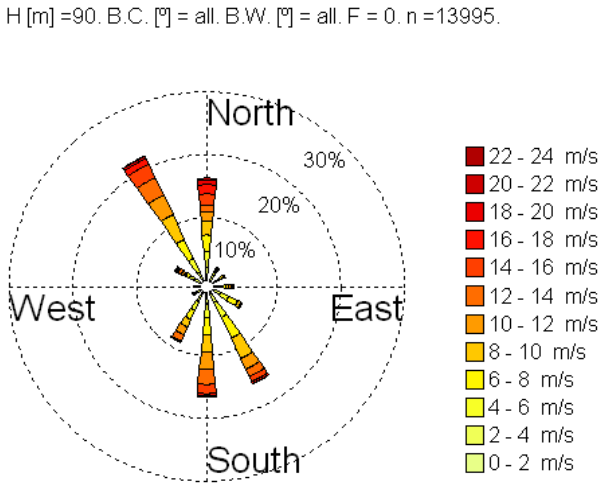

Figure 2-2. Wind direction frequency distribution. Wind speed distributions indicated by color scale.

Now with a better understanding of the general wind conditions present during the measurement period, it is possible to proceed analyzing the measurements and compare the lidar performance with the standard cup anemometry. This is done in the following sections, starting with an overall visualization of the wind speed time series.

2.3 Time series

The total of the wind speed records for the measurement campaign is shown in Table 2.3-1 for the two lidar devices. In gray color appear all the simultaneous data recorded by the two lidars and the met mast at 90 m height. Some filtering criteria for the met mast instrumentation are applied, as indicated in the "Comments" column. They are the ZephIR's Scans in Average (S_{av}), the Points in Fit (P_f), the Turb parameter (T_b), the Scaling factor at 38 m height (S_{38}), the Windcube's Availability (A_v), the met mast measurements of the horizontal wind speed (U), the ambient temperature (T), the rain detector (R_a) and the wind direction (θ).

Then, additional filtering parameters are applied to each of the lidar devices according to the different variables they log during operation. These filters help to reduce the number of records where the lidar measurements are very likely to be erroneous. The resultant dataset correspond to the black circles for the cup anemometer data and the green crosses for the respective lidar in figures of Table 2.3-1.

Table 2.3-1. Time series for the horizontal wind speed during the measurement campaign, at 90 m height. The black circles represent the filtered cup anemometer measurements and the green crosses represent the filtered lidar data. The gray markers correspond to the unfiltered data set for each sensor. Only simultaneously available data from both sensors are accounted.

	Complex terrain	Comments
ZephIR	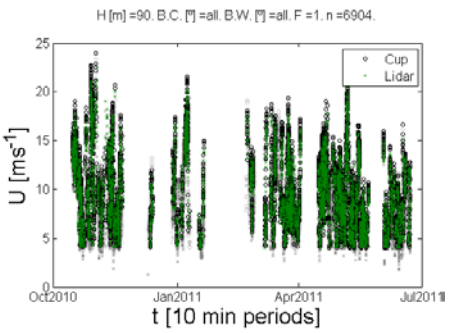	Lidar filters: S_{av} >= 50 P_f >= 35 T_b < 0.10 S_{38} >= 50
Windcube	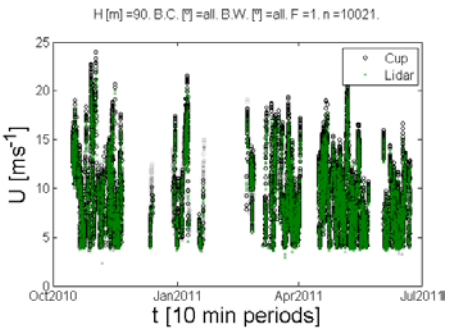	Lidar filters: A_v = 100% Mast filters: U >= 4 ms^{-1} T > 2 ºC R_a = no rain θ = all

Notice that the resultant filtered time series present some considerable gaps and therefore the records are not equally distributed during the measuring periods. This is important to take into account since the atmospheric conditions vary from season to season and this could have an impact in the measurements averages. Thus, the atmospheric conditions should be well characterized and understood in order to help derive conclusions from the lidar error analysis.

In this same line of reasoning, there is a necessity to assess the data availability before and after applying the indicated lidar quality filters. This gives an indication of the representativeness of the final dataset and also helps to identify what are the main factors that reduce the availability of good quality lidar data. In section 2.4, the data availability for the measurement campaign is detailed.

2.4 Data availability

Several quality filters have been applied in order to eliminate erroneous or obviously corrupted lidar and cup anemometer data. Nevertheless, it is important to assess the amount of records that are lost on each case since in order to achieve relevant conclusions, a statically representative amount of data is necessary.

Regarding the data filtering criteria, there are some variables in common and some others very specific for each kind of device. For the cup anemometer data, the first filtering criterion is that the ambient temperature must be higher than 2 ºC to avoid frozen or retarded anemometers. Also, only wind speeds higher than 4 ms^{-1} are considered due to the ZephIR operation range and also because the calibration range of the cup anemometers (Pedersen,

2006). The higher limit of the cup calibration range is normally 16 ms^{-1}, however data above this limit was still considered in order to assess the lidar performance at these higher velocity values.

The periods where rain was present are discarded since rain is likely to introduce a vertical speed component that affects the lidar measurements. This happens when the backscatter coming from falling drops is interpreted by the lidar as a downward component, which is incorrect in this case (Antoniou, 2006). Moreover, if very heavy rain is present, the laser beam can be blocked at the lidar window.

Additionally, each lidar registers several signals apart from the measured wind speed. These signals offer the chance to filter out the data based on the specific device properties. For instance, at each 10-min period, the ZephIR records the number of circular scans at each height that are accomplished during each 10-min period. A minimum amount of scans is selected to assure that enough data was recorded and the 10-min period average is representative of the wind conditions during that period. Since the ZephIR is scanning one revolution (one second) per height at each of the 5 heights, a minimum value of 50 scans-in-average per 10 minute period is chosen as a quality filter.

Moreover, the average number of radial velocities retrieved at each circular scan is used as a filter for the 10 minute periods. This parameter is known as the points-in-fit. and indicates whether or not there was sufficient backscatter from the atmosphere from all directions. This is important since the ZephIR's processing algorithm performs a fit to a rectified cosine function. If there are too few points, the uncertainty of the fitted function increases. A minimum requirement of 35 (out of 50 possible when scanning once per height) is selected as a data filter. These thresholds are based on the experience accumulated at CENER after several years working with the ZephIR lidar.

For the ZephIR, there is an additional parameter that helps to identify the goodness of the fitting function. The turb (T_b) parameter indicates how much deviation there was in general from the measured points to the estimated function to be fitted. The T_b parameter gives information with resemblance to what in statistics offers the sum of squared residuals. Consequently, higher values of the T_b parameter can be an indication of considerable non-uniformity of the wind velocity field where the ZephIR was scanning. This can help to identify very turbulent wind flows. Additionally, the T_b parameter can be an indicator of noise in the retrieved signal. For this study, only datasets where the T_b value was 0.1 or less have been taken into account.

Furthermore, the ZephIR's scaling factor is a parameter related to the strength of the backscattered signal. It is the scaling factor that resulted from the conversion of the initial Fast Fourier Transform (FFT) float values to the actually saved values which are byte scaled (8 bits). This means that the recorded values have to be divided by the scaling factor in order to obtain the original values: $FFT\_\max \cdot Scaling = 255$. Thus, a strong backscatter signal returns a lower value of the scaling factor if compared to a weak signal that would require a higher scaling value. Normally, weak signals are the result of very clear air where low aerosol concentration backscatters just a small proportion of the emitted laser energy. On the other hand, a low scaling factor value indicates that the returning signal was strong enough to be easily detected. This is caused by the presence of higher aerosol concentration.

It has been seen that the presence of fog or low clouds gives rise to an abnormally intense backscatter. For our interest, this situation can be quantified based on the scaling factor values. In general, a scaling factor higher than 50 from the lowest measuring height (38 m as default) can help to filter out periods with high presence of foggy conditions. For the case of

Alaiz test site, since it is a rather high mountain surrounded by flatter regions, the ambient vapor frequently condenses around its top, causing foggy conditions, especially during winter months.

In respect to the specific Windcube data filtering criteria, this is basically reduced to the device availability. This parameter indicates how much of the time during each 10-min period, the received backscatter was above a pre-defined threshold level and the device was thus able reconstruct a horizontal wind speed. Fog, low cloud and obstructions (rain) can result in lower than 100% availability. In this study, only periods with 100% lidar availability were selected for analysis.

Differently to CW lidars such as the ZephIR, the Windcube is a pulsed lidar. The main difference in the working principle is that CW lidars sense the signal backscatter constantly. The main assumption is that the returning signal comes from the desired measuring height which is achieved by using a lens to focus the laser energy there. If the signal is actually backscattered from a different height, there is not a direct way to detect it. In contrast, the pulsed lidar emits a signal pulse of a specific length and calculates the time necessary to reach and return from the desired measuring height, sampling the backscatter at this time. During this sampling window, only backscatter from the desired range can physically be detected. These two sensing approaches have both advantages and disadvantages as have been previously discussed by Wagner (2010).

As a final filtering criterion that in general affects the performance of all the devices is the presence of obstacles that obstruct the free wind flow and can produce wind acceleration or form wakes with considerable wind speed reduction and increased turbulence intensity. The first example is the presence of the met mast itself that directly affects the flow with distortions that reach the cup anemometer location. It is necessary to filter out data based on the wind direction in order to reduce as much as possible the met mast effects. It has been seen that the mast wake effect differs depending on the mast structure. Additionally, for those wind directions where there is no direct wake incidence on any of the cup anemometers, the mast effects are still noticeable. For instance, if plotting the ratio of two cup anemometers (at the same height but at opposite sides of the met mast) as function of the wind direction, a kind of sinus wave shape reflects how the flow is disturbed by the mast presence. This information could be used to “correct” the cup anemometer measurements in order to reduce the mast effects (Lindelöw, 2010). Nevertheless, this approach has not been performed for the present study.

Another aspect to be taken into account when selecting the wind direction sectors to be used for the lidar-cup correlation is the presence of any large structure nearby.. These structures can produce strong wind turbulence or flow obstruction at several scales affecting differently the cup anemometers and the lidars.

For each of the mentioned filters, the resultant data availability is presented in Table 2.4-1. The column *Description* indicates what the filtering criteria used are and the column *Purpose* explains the purpose of applying such filters. The base number of records is 11555 which are those records where the cup anemometer and the two lidars were working simultaneously and recording wind measurements from a valid direction sector. Notice that the main factors that reduce the available data are the Windcube availability and ZephIR scaling factor at 38 m. These are precisely indicators of the presence of low clouds or fog that obstruct the transmission of the laser beam and therefore there is no backscatter to sense for the case of the pulsed lidar or there is too much backscatter at the lowest measurement height for the case of the CW lidar.

Furthermore, it is important to mention that the measurement campaign at Alaiz has been performed during the winter months. This implies the presence of adverse conditions since the cup anemometers and wind vanes can get frozen more easily and also the presence of clouds and mist is more frequent. In order to filter out possible full or partially frozen anemometers, as already mentioned, a filter of minimum ambient temperature of 2 ºC has been used during the previous analysis. Notice that just due to this filter, 23% of the data are filtered out. By combining all the filters together, the final result is a data availability of 29%. This means that the different filtering criteria are affecting in different manners the wind sensing devices used during the campaign.

Table 2.4-1. Data availability after applying several data quality filters. Alaiz measurement campaign at 90 m height.

Filters				Availability	
Device affected	*Condition*	*Description*	*Purpose*	*Number of records*	*Percentage*
All	Time synchronization	Dataset with synchronized measurements from the met mast and the two lidars operating simultaneously	Compare the equipment only in those periods when the three sensing devices were active and working properly	11555	100%
Met mast	Wind direction: North +/- 45 º and South +/- 45 º	For the site location, one or more valid wind direction sectors are carefully chosen. This is the starting point to compare all the sensing devices	To avoid the presence of big nearby obstacles, wind turbine wakes and specially the met mast effects (flow distortion over the wind reaching the cup anemometers)	9781	85%
	Temperature > 2 ºC	The ambient temperature should be on average higher that 2 ºC during each 10 minute period	To avoid frozen anemometers and wind vanes, a minimum ambient temperature is used to filter the erroneous data	7778	67%
	u >= 4 m/s	The horizontal wind speed should be on average higher than 4 m/s during each 10 minute period	The calibration range for the cup anemometers is from 4 m/s to 16 m/s. Also to avoid the inertial effects and eventual frozen periods, the minimum limit is used to filter data	10436	90%
	No rain	Avoid rainy periods	Prevent introduction of a dowards vertical component in lidar measurements as well horizontal speed memory from higher heights	8794	76%
Windcube	availability = 100%	Considers only 10 minute periods where the Windcube was able to measure 100% of the time	Assure the device was able to measure at the desired height all of the time	8264	72%
ZephIR	Scans in average >= 50	The number of circular scans per height for each 10 min period should be at least 50	Assure to have nearly full measurement availability from the desired height	10050	87%
	Points in fit >= 35	The number of radial velocities adquired from each circular scan should be on average at least 35 during each 10 minute period	Take into account only measurements with enough radial velocities to make a good cosine function adjustment to determine the wind vector	10589	92%
	Turbulence parameter < 0,1	The Turb parameter (dispersion of the radial velocities from the adjusted cosine funtion) should be on average lower than 0.10 during each 10 minute period	Avoid measurements where there was high spatial variation of disperssion of the radial velocities	10778	93%
	Scaling at 38 m >= 50	The scaling parameter for the backscatter retrieved from the 38 m height measurements should be on average higher than 50 during each 10 minute period	In order to filter out measurements with high probability of fog presence, only measurements with not very strong backscatter from the lowest measurement height are used	7304	63%
All	All filters together	All the met mast and the specific lidar in study applied sumultaneously	To assure good data quality from all the sensing devices and make representative comparisions between their measurements	3477	30%

The available records per wind direction, after applying the met mast filtering criteria are shown in gray lines Table 2.4-2. If additionally, the lidar and met mast filtering criteria are applied, the resultant amount of records is shown by the black lines. Within these filtering criteria, the called “predominant” wind direction refers to the predominant wind direction based on long term measurements previously studied at each test site (which might differ from the wind rose results presented in section 2.2 that consider only the measurements taken during the current experiment). Special care was additionally taken about avoiding wind

direction sectors where big structures obstruct the free wind flow, including the met mast wake itself.

After applying these filters at the complex terrain site, most of the available records are registered mainly at the north-south axis, while the western sector is almost empty of data points. This information was taken into account when the met masts were installed in the test site in order to align the boom directions perpendicular to the predominant wind directions with the purpose of minimizing the mast effects over the cup measurements.

Table 2.4-2. Distribution of the dataset per wind direction at 90 m height. Example for the Windcube lidar. In light gray dots the mast-only filtered dataset and in black dots the mast-and-lidar filtered dataset.

Complex terrain	Comments
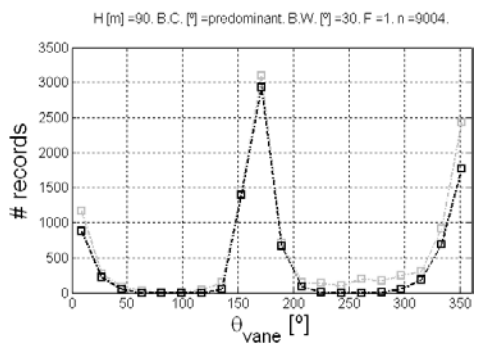	Lidar filters: A_v = 100% Mast filters: U >= 4 ms^{-1} T > 2 ºC R_a = no rain θ = obstacle and mast wake free sector

From Table 2.4-1, it is possible to quantify the incidence frequency of some conditions that are known to be indicators of poor lidar measurements. In order to quantify the magnitude of the average error reduction that can be achieved by filtering the dataset based on these indicators, a general analysis of lidar performance in complex terrain is conducted.

2.5 Horizontal wind speed correlation from lidar and cup anemometer measurements

As indicated above, the reference wind speed is taken as the one given by the cup anemometer at the corresponding measurement height. The lidar and cup anemometer inter-comparison has been done using measurements at 90 m height, unless indicated otherwise.

Firstly, the correlation of the measured horizontal wind speed U between cup anemometer and the lidars is presented in Table 2.5-1. As can be seen, the ZephIR and Windcube measurements for the horizontal wind speed are compared with those from cup anemometers. Notice in the figures, the correlation is generally good once some data quality filters have been applied. In order to visualize the effects of filtering, the unfiltered data are represented as light gray dots and the filtered data correspond to the darker dots. The sources of error in the lidar measurements will be explained in the coming section.

Table 2.5-1. Correlation of horizontal wind speed *U* between lidars and cup anemometer at 90 m height. In light gray dots the overall unfiltered dataset and in black dots the filtered data. The lidar data filters applied are indicated in the "Comments" column.

	Complex terrain	Comments
ZephIR	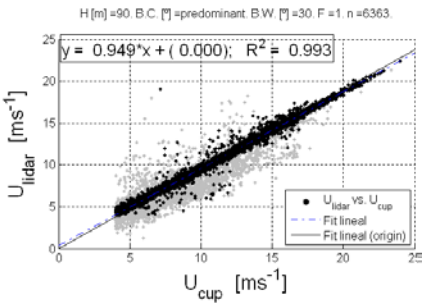	Lidar filters: S_{av} >= 50 P_f >= 35 T_b < 0.10 S_{38} >= 50
Windcube	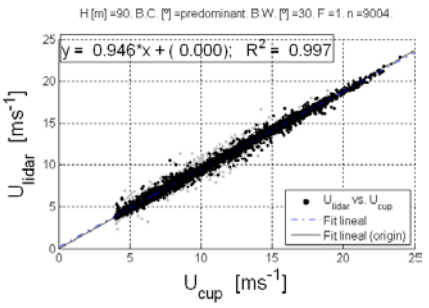	Lidar filters: A_v = 100% Mast filters: U >= 4 ms^{-1} T > 2 ºC R_a = no rain θ = obstacle and mast wake free sector

Despite applying the mentioned filters, there still exists some dispersion in the correlation graphs. A first attempt to identify the main lidar error sources affecting the lidars in complex terrain is introduced in the next section.

2.6 Lidar error sources

1.1.3 Introduction

When facing the task of assessing the lidar performance, it is necessary to identify what are the main sources of error between lidar and cup anemometer measurements. This is not an easy task since diverse variables can affect cups and lidars differently and some others can affect them similarly. Ideally, it should be possible to identify the individual effect of each variable over each device, however some error sources can appear simultaneously and therefore separating their influence becomes a difficult assignment. The main sources of lidar error can be classified into several groups as shown in Figure 2-3.

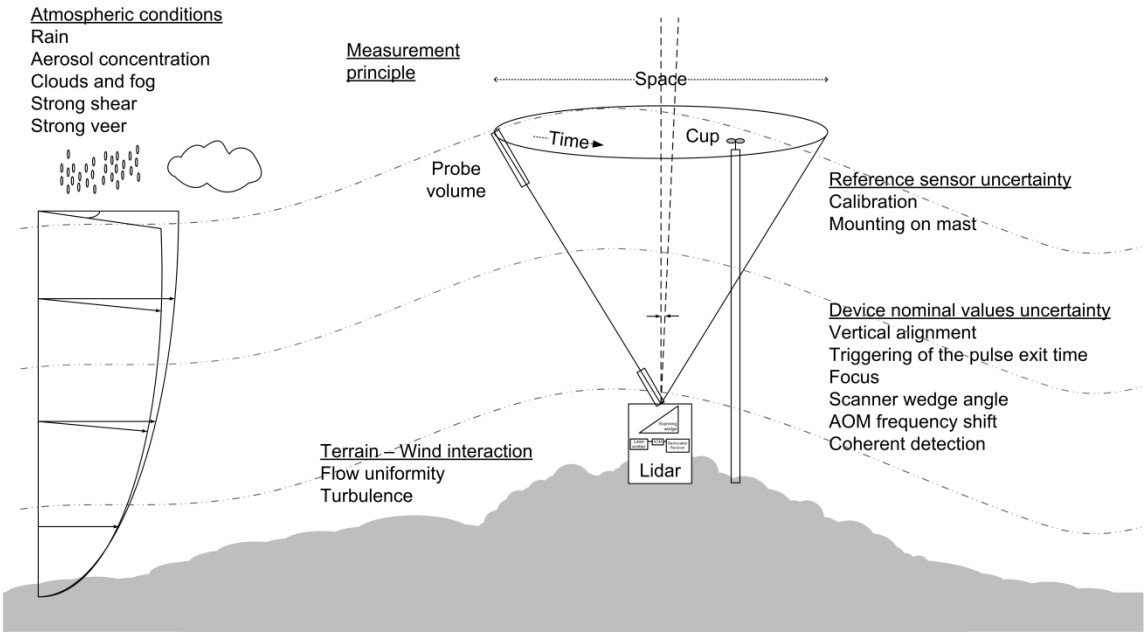

Figure 2-3. Lidar error sources.

The scope of this report is to identify the sources of lidar error caused by external agents, i.e. no research is taken on the hardware functioning or internal signal processing properties attained by each device. These external agents can be classified into two main categories: those related to the atmospheric conditions and those related to the terrain complexity.

Since the main interest of this research work is to evaluate the terrain complexity influence on the lidar measurements, it is therefore important to separate as much as possible the erroneous lidar records caused by atmospheric conditions. Based on previous studies at Alaiz, it was found that the presence of ground fog and also low clouds are relevant sources of lidar uncertainty. For that reason, it is of high significance to filter out these conditions as much as possible before studying the terrain effects on the lidar performance. This approach is explained in coming sections.

1.1.4 Cloud correction algorithm for the ZephIR lidar

The cloud correction algorithm for the ZephIR lidar is implemented using the scaling factor signals from two additional heights at which the ZephIR measures apart from the 5 heights selected by the user. These heights are 38 m and 800 m. In figures from Table 2.6-1, the influence of two different scaling factors over the lidar error is shown.

Table 2.6-1. Lidar error and scaling factors at 38 and 800 m for the ZephIR lidar at 90 m height. In light gray dots the overall unfiltered dataset and in black dots the filtered data.

	Complex terrain	Comments
Scaling at lowest height (SL)	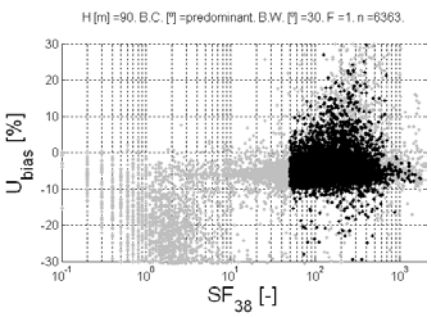	Lidar filters: S_{av} >= 28 P_f >= 105 T_b < 0.10 Mast filters: U >= 4 ms^{-1} T > 2 ºC R_a = no rain θ = obstacle and mast wake free sector
Scaling at highest height (SH)	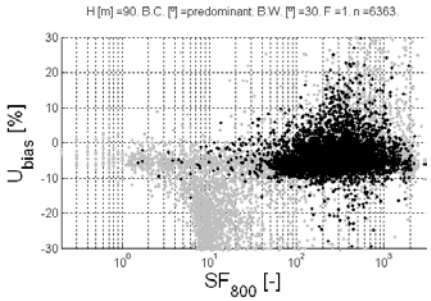	
SL / SH	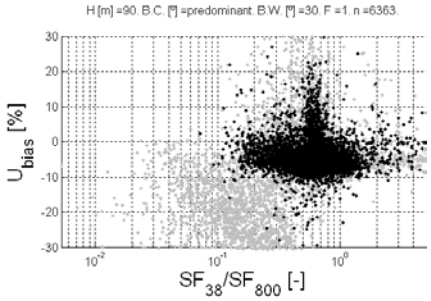	

Since there is such a high frequency of fog at Alaiz, the scaling filter > 50 was not applied, but the fog filter implemented by the manufacturer was emulated. Considerable scatter in the lidar relative error is still observed and therefore for the Alaiz test site, a filter of the scaling parameter from 38 m height > 50 is chosen as a reasonably good filter criterion to reduce the lidar error. As indicated, most of the remaining figures concerning the ZephIR presented in this document have been plotted with this filter giving reasonably good results.

1.1.5 Wind direction: examining the site surrounding conditions

The influence of the terrain conditions can be revealed when plotting lidar error as a function of the wind direction, as shown in the graphs from Table 2. At the complex terrain site Alaiz, observe that the wind blows mainly from north (at 0º with uphill wind) and south (at 180º and downhill wind) directions. It has been seen in previous studies that at the mountain top, the lidars tend to underestimate the wind speed (the error is mainly negative). Nevertheless, for the region between 180º and 360º, there are enough data to identify a curve shape in the plot revealing the terrain effects, since for the west and east directions, the mountain top is flatter and less flow curvature is expected. This is seen in the lower lidar underestimation of the

horizontal wind speed for this direction sector. The lidars tend to underestimate the wind velocity from northern and southern sectors, precisely where there is more curvature in the flow due to the alignment with the mountain slope.

Table 2.6-2. Lidar horizontal velocity error vs. wind wane direction at 90 m height. In light gray dots the overall unfiltered dataset and in black dots the filtered data. Bin averages and standard deviations indicated by squares and error bars.

	Complex terrain	Comments
ZephIR	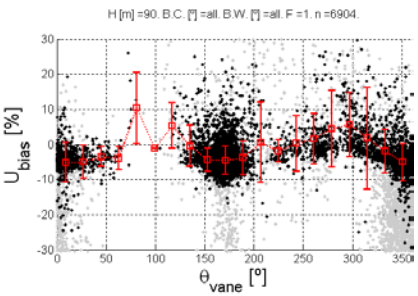	Lidar filters: S_{av} >= 50 P_f >= 35 T_b < 0.10 S_{38} >= 50
Windcube	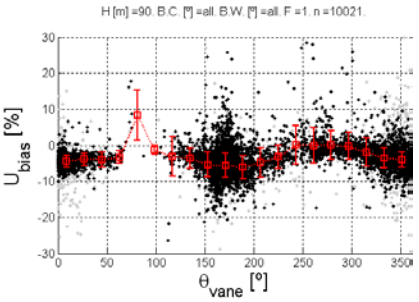	Lidar filters: A_v = 100% Mast filters: U >= 4 ms^{-1} T > 2 ºC R_a = no rain

For wind direction where the wind flows parallel to the flat mountain top (eastern and western sectors), the lidar error is apparently reduced. At 270º there is a group of data revealing the mast effect. Here the cup anemometer might be sensing a reduced wind speed due to the wind flow obstruction caused by the mast.

1.1.6 Mast effects

The mast effects over the wind sensing instrumentation installed on it, comes from the wind flow obstruction that the mast presence introduces. Anemometers installed in booms aligned with the wind flow and the mast either sense the blocked wind flow before it approaches the mast or senses the mast wake behind the mast (Jaynes, 2007; Lindelöw, 2010). In Figure 2-4, this effect is illustrated for the case of the MP5 met mast at the Alaiz test site.

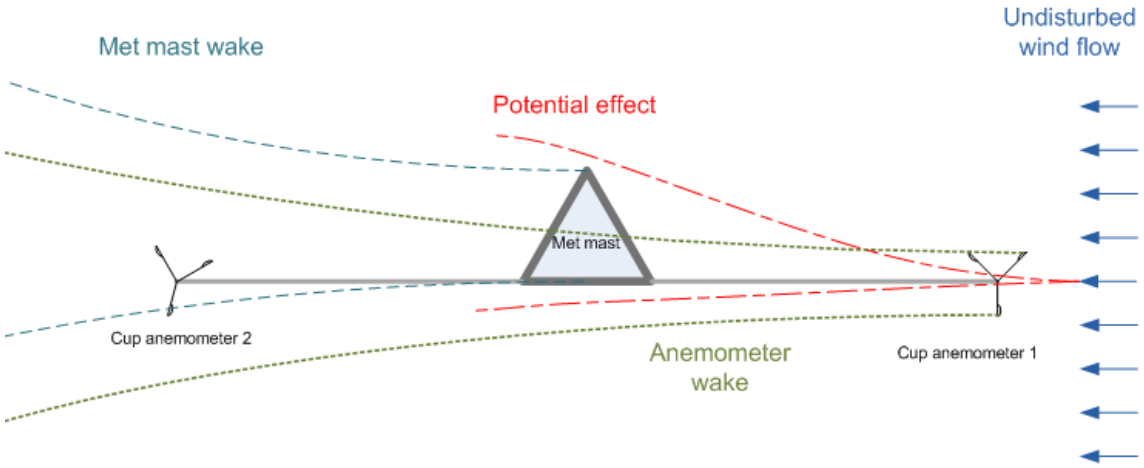

Figure 2-4. Met mast effects on anemometer measurements.

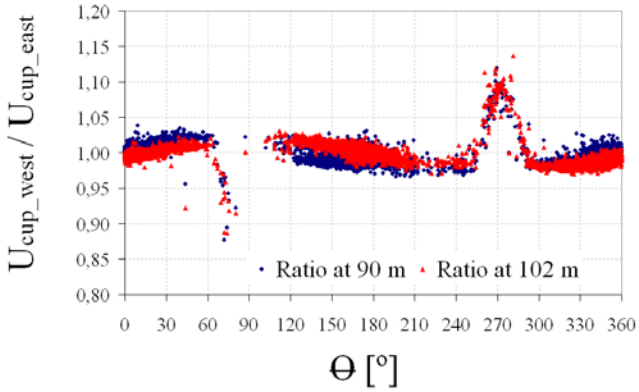

Figure 2-5. Cup anemometer wind speed ratios (west speed/east speed) for measurements at 90 and 102 m height.

The ratios of the wind speeds measured by the anemometers in the Alaiz mast are plotted in Figure 2-5 as a function of the wind direction. It is noticeable that the mast wakes account for the highest wind speed deficit sensed by the anemometers. Nevertheless, observe that the other mast effects apart from those in region of the mast wake, can account up to 5% of uncertainty in the anemometer measurements. Despite the fact that the instrumentation was installed following strict standards and recommendations, these undesired effects are difficult to avoid. It is clear that not all the sources of lidar error are due to the lidar devices themselves, but also due to uncertainty arising from the installation of the cup anemometers, which is considered as the reference instrument.

1.1.7 Tilt angle, vertical velocity and vertical velocity gradient

Additionally to the horizontal component of the wind vector, the lidars are also able to determine the vertical component *w*. At the complex terrain site in Alaiz, the mast has vertical propeller anemometers installed at several heights. The two graphs at the right of Table 2.6-3 show the lidar error of the vertical wind velocity at 118 m height. The reason for using this height instead of 90 m as previously is the poor data availability from the propeller at 90 m. In this set of graphs it is difficult to identify a clear behavior due to the scatter in the plots. However, observe that when wind blows from south (in a range approximately from 140º to 180º) the lidars tend to overestimate the vertical component (with negative magnitude in this case). Contrary, when wind blows from north, the lidars seem to underestimate the vertical

component, and therefore the error is negative too. The gap in the data from around 50º to 120º is simply because there is almost no wind blowing from that sector at this location. The wind rose is very north/south directional for Alaiz.

Table 2.6-3. Lidar vertical velocity error vs. wind wane direction at 118 m. In light gray dots the overall unfiltered dataset and in black dots the filtered data. Bin averages and standard deviations indicated by squares and error bars.

	Complex terrain	Comments
ZephIR	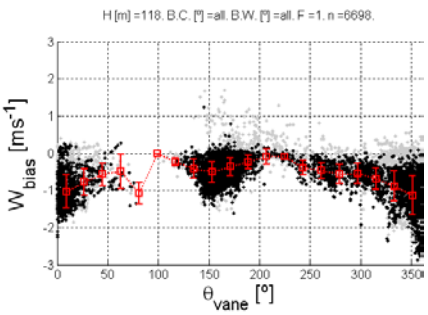	Lidar filters: S_{av} >= 50 P_f >= 35 T_b < 0.10 S_{38} >= 50
Windcube	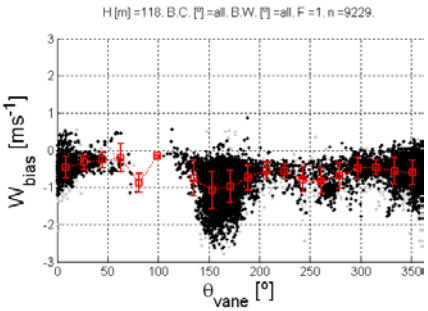	Lidar filters: A_v = 100% Mast filters: U >= 4 ms^{-1} T > 2 ºC R_a = no rain

Remember that the lidars and the mast are installed precisely at the mountain edge where the northern uniform slope gives place to a flatter hill top. So the lidar beams are sensing radial velocities above an inclined surface to the north and above a flat surface to the south. This result in measuring different wind vectors assuming the wind flow follows the ground contour as in left figure from Table 2.6-4. Besides, it is important to mention that the Windcube vertical component is recorded with the opposite sign to the ones registered by the ZephIR and the propeller anemometers (Antoniou, 2006). For this reason the Windcube value of $-w$ has been used instead.

Several authors have pointed out that the main lidar source of uncertainty in complex terrain conditions is the vertical wind speed gradient (Bingöl, 2009; Boquet, 2010). To verify this hypothesis, the lidar horizontal velocity error is plotted as a function of the vertical velocity (not the gradient since it is not possible yet to estimate it from the available sensors at Alaiz) in figures from Table 2.6-4. As explained above, since the lidars are installed at the mountain edge, this is precisely the location where the highest vertical speed gradient is expected. This reasoning can be supported with results from another experiment where a scaled mock-up of the Alaiz mountain has been studied in wind tunnel experiments (Boris et al., 2011). For the preliminary results of the wind flow aligned with the north-south direction, see the graphs from Figure 2-6. These two dimensional graphs show the wind properties measured along an axis over the model which passes in the proximity of the met mast and lidar location at the hill top. The relative alignment of the lidar and met mast location with respect of the axis is

indicated by the dotted line. As can be seen, the highest wind acceleration and vertical wind speed gradient happens in the hill region where the lidars and met mast are installed.

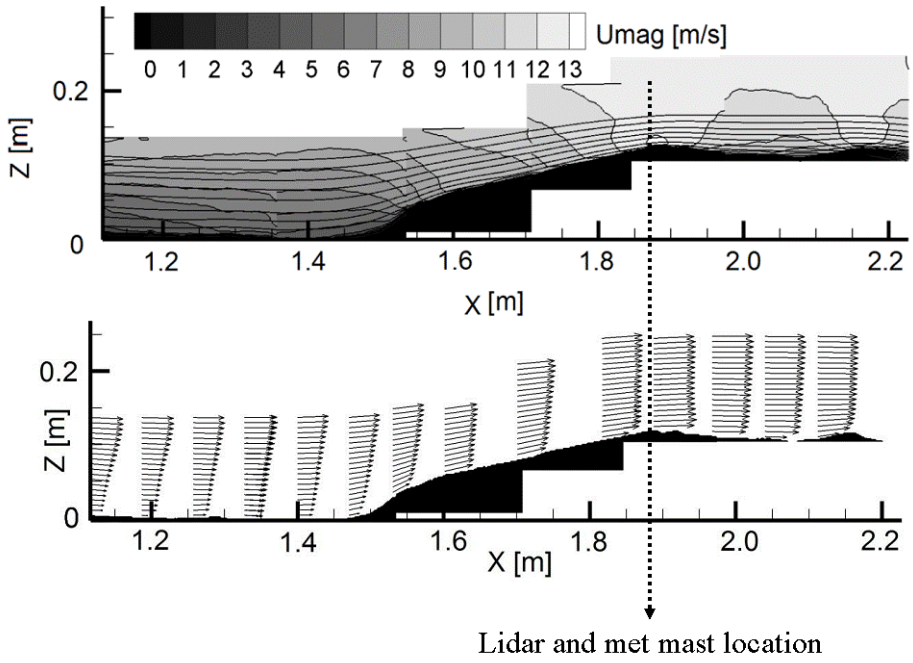

Figure 2-6. Mean velocity and vector field extracted from PIV results. Adapted from Boris et al. (2011)

Despite the fact that the wind tunnel experiments reproduce very specific conditions from the atmosphere, these results are helpful to understand the wind flow over the Alaiz mountain and predict the lidar performance when installed at different locations.

1.1.8 Terrain effects

In order to assess the terrain effects from the Alaiz mountain, a starting point is to plot the lidar error as a function of the vertical component of the wind velocity. The results are shown in figures from **Erreur ! Source du renvoi introuvable.**. Similar results are obtained using the tilt angle instead as will be shown afterwards.

Table 2.6-4. Lidar horizontal velocity error vs. propeller vertical velocity at 118 m height. In light gray dots the overall unfiltered dataset and in black dots the filtered data. Bin averages and standard deviations indicated by squares and error bars.

	Complex terrain	Comments
ZephIR	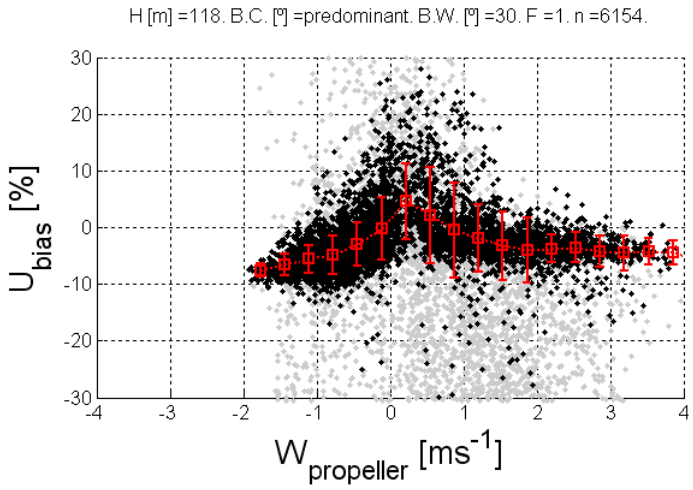	Lidar filters: S_{av} >= 50 P_f >= 35 T_b < 0.10 S_{38} >= 50
Windcube	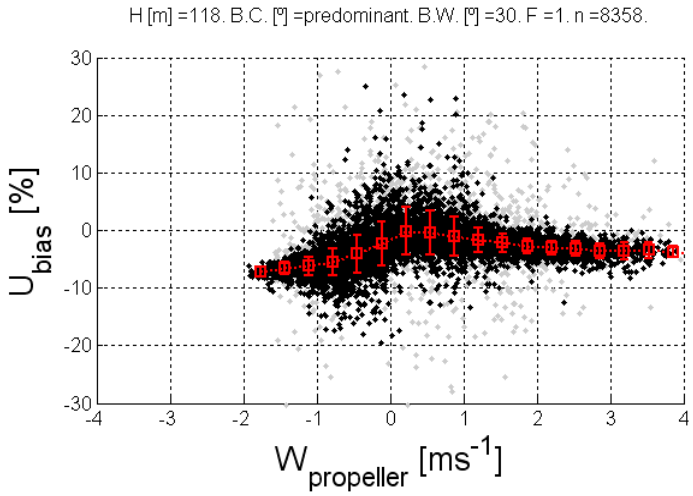	Lidar filters: A_v = 100% Mast filters: U >= 4 ms^{-1} T > 2 ºC R_a = no rain θ = obstacle and mast wake free sector
	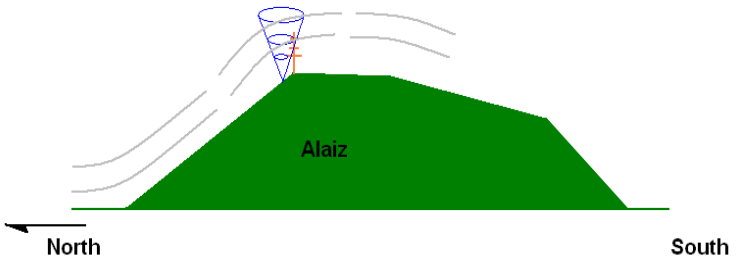	

From the plots it is clear that as the vertical velocity component *w* increases in magnitude, the lidars tend to underestimate the horizontal wind speed. The two graphs show very concise information about the difficulty of lidar systems in measuring the true horizontal wind speed in sloping terrain. Very similar results are obtained if the tilt angle is used instead of *w*. Different slopes are observed whether the wind is blowing uphill (coming from north) or downhill (coming from south). The reason of this behavior is not totally understood yet and further analysis is needed. A likely explanation is that the change in tilt angle between the

lidar upstream and downstream measuring volumes, scales with the magnitude of the vertical speed. From the theory, we understand that it is the change in tilt angle that is the cause of the lidar error.

The tilt angle obtained from the vertical and horizontal anemometers and the one measured by the lidar is shown in Figure 2-7. The lines indicate the absolute value of the tilt angle differences.

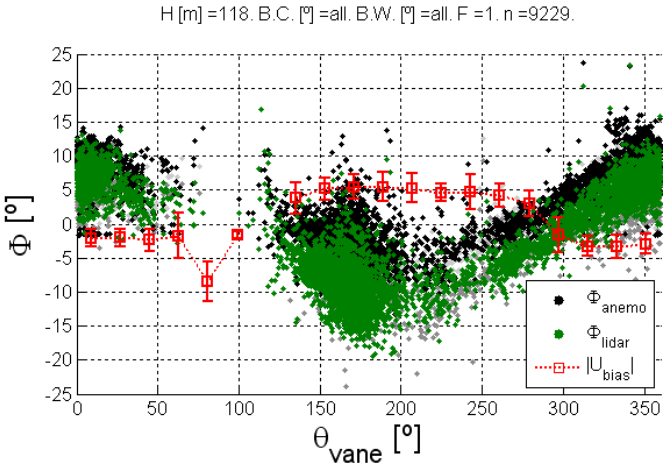

Figure 2-7. Wind flow tilt angle for all wind directions. Example for the Windcube lidar at 118 m height at the complex terrain site. In light gray dots the overall unfiltered dataset and in black dots the filtered data. Bin averages and standard deviations indicated by squares and error bars.

In previous paragraphs, the influence of non-uniform wind flow was indicated to play an important role in lidar uncertainty. Since cup anemometer measurements represent just a point in space, it is not possible to directly obtain information about the wind flow uniformity from the reference instrumentation. This kind of information can be indirectly obtained from numerical flow models.

3. Description of the sodar campaign

The site of campaign and the instrumentation are described in detail in the deliverable Dc2.3 Overview of the SAFEWIND project [17].

Three remote sensing instruments were used during the SAFEWIND campaign:

- A Leosphere WindCube WLS7 lidar from RISOE (pulsed emission)
- A Qinetiq Zephir lidar from CENER (continuous wave)
- A Scintec SFAS sodar from EDF-R&D.

The WindCube is a pulsed lidar with a fixed focus and with 4 beam directions. It is able to provide wind vertical profile approximately each 1.5 s. It allows for the possibility of obtaining wind measurements at up to ten different heights ranging between 40m and 300m. In this campaign it was configured to measure at 40m, 78m, 90m, 102m, 118m, to match relevant mast instrumentation, and additional heights of 130m, 200m, 250m and 300m. This lidar was collocated with MP5 mast (figures 3-1 and 3-2), except between 8 March and 12 April 2011. During this period, it was collocated with the sodar.

In the intercomparison involving the sodar, Zephir data were not used.

The configuration of the sodar is summarized in table 3-1.The pulse duration was 5 m for the highest frequencies, and 15 m for the lowest frequencies. The sodar was located at 220 m West from MP5 mast (figures 3-2 and 3-3). This distance was expected to be large enough to avoid ground clutter effects from the mast. Taking into account the prevailing wind directions and the possible fixed echoes, the antenna azimuth was set to 44°.

Number of frequencies	10
Range of frequencies	2500 to 4900 Hz
Number of beams	9
Period of integration	10 min
Pulse duration (m)	5 to 15 m
Height range of measurement	10 to 150 m
Output vertical resolution	5 m

Table 3-1: Sodar parameters during the Alaiz campaign.

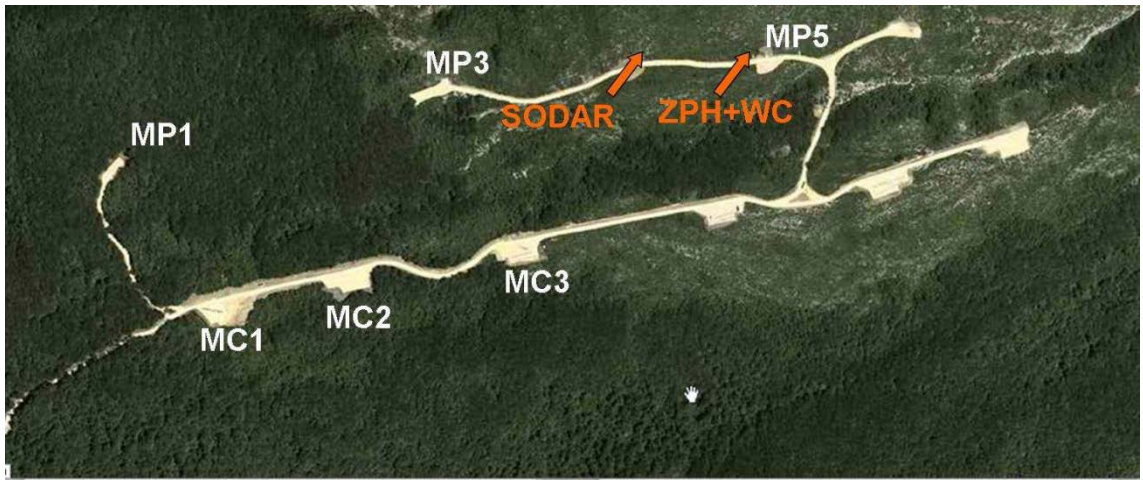

Figure 3-1 – Aerial view of the test station during the second phase of the campaign. Positions of sodar, ZephIR ("ZPH") and WindCube ("WC") and meteorological masts (from [1]).

Figure 3-2 – Deployment of lidars in Alaiz and reference meteorological mast MP5 (from [1]).

Figure 3-3 – Sodar and reference meteorological mast MP5 (from [1]).

Concerning the sodar the main events during the campaign were:

- 13-15 October 2010: installation
- 15 October to 20 December: Sodar worked well except on 4 and 6 November
- 20 December to 31 January:
  - ✓ Problem with loudspeaker 27 showed by antenna test (all the row was affected)
  - ✓ Bad electric connection, but not permanently
- 31 January: loudspeaker 27 disconnected

- 31 January to 8 March: antenna OK, good data availability, still some problems of electric connection
- 8 March to 12 April: sodar and Windcube collocated
- 20 April: new power supply cable --> improvement of data availability
- 30 June: end of measurements

4. Comparison between sodar and MP5 mast

4.1 Selection of the data set

Data from the period between 20 December 2010 and 31 January 2011 have been removed because of antenna problem mentioned above.

Period P1 is defined as the merge of: 15 October to 20 December 2010, 31 January to 8 April 2011, and 12 May to 12 June 2011. Period P2 is the period between 8 April and 12 May 2011. Period P is defined as the merge of P1 and P2.

The data set for the inter-comparison has been defined in order to be also suitable for the analysis of vertical profiles presented in section 4.2. Thus, only complete vertical profiles have been selected. Although data have been obtained up to 150 m and SFAS sodar data have shown during previous campaigns that they were reliable from level 30 m, the minimum and maximum heights have been set to 40 m and 120 m respectively, in order to maximise the number of selected profiles while covering the whole range covered by actual turbine rotors.

The comparison between the sodar and MP5 has been performed on P1, selecting only the relevant data for wind energy purposes, i.e. for which the MP5 wind speed at 80 m is higher than 3 m/s.

As for the campaign in flat terrain (deliverable Dc-2.2 assessment), the effect of different additional filters on the statistical scores of this comparison has been studied, based on different indicators provided by Scintec software (except for the rain):

- Data obtained in presence of rain;
- Data obtained when the backscattering intensity is set by the software at its default value (this is the case when the peak due to the wind in the Doppler spectrum is not well defined);
- Data associated with invalidated standard deviation (of one of the horizontal components);
- Data associated with a confidence class < 3 for one of the 3 components of the wind (on a scale ranging from 1 to 4);
- Data associated with an error code = 256 (presence of ground clutter contamination but which has been removed by the manufacturer software);
- Data associated with an error code = 258 (presence of ground clutter contamination with invalidation of vertical wind).

These filters applied individually or combined in different ways did not show any significant modification in the statistical scores of the comparison between the sodar and the MP5 mast. In particular, as during the Høvsøre campaign, no significant difference was observed when rain cases were removed: it confirms (over a much longer period than at Høvsøre) that the Scintec SFAS sodar is very weakly affected by rain. Finally, the comparison was made using only the filter on the confidence class, because it allowed to remove some cases of large sodar errors. It had no significant impact on the statistical scores (only 1.3 % of the data removed) but it was considered as useful in view of the further data analysis for the deliverable 2.4 (profile classification). Thus, the comparison was made over 13 558 time samples.

4.2 Inter-comparison results

The scatter plots at 40 m, 80 m, and 120 m are shown on figure 4-1. Statistical scores are summarized in table 4-3, which includes a comparison between northern winds and southern winds. The best results are obtained at 40 m where the error is lower than 0.1 m/s, and the regression slope indicates an underestimation of about 1.5 %. At 80 m and 120 m, the error remains lower than 0.3 m/s and there is an underestimation of about 3.5%. The correlation coefficient lies between 0.97 and 0.98 at 3 levels.

A careful analysis of the backscatter plot (raw data) for the different wavelengths and different beams did not show any obvious sign of fixed echoes (figure 4-2), contrary to the Høvsøre campaign. This is

consistent with the analysis on which was based the choice of the sodar location. Thus, the wind speed underestimation by the sodar seems to be due in this case to an effect of the topography.

The underestimation is less pronounced for northern winds (315° to 45°) than for southern winds (135° to 225°), especially at 120 m, which can be explained by the different topography on North and South sides of the ridge.

Finally we can note that the sodar is able to measure winds up to more than 22 m/s (with an integration period of 10 minutes), although a systematic underestimation is observed above 18 m/s.

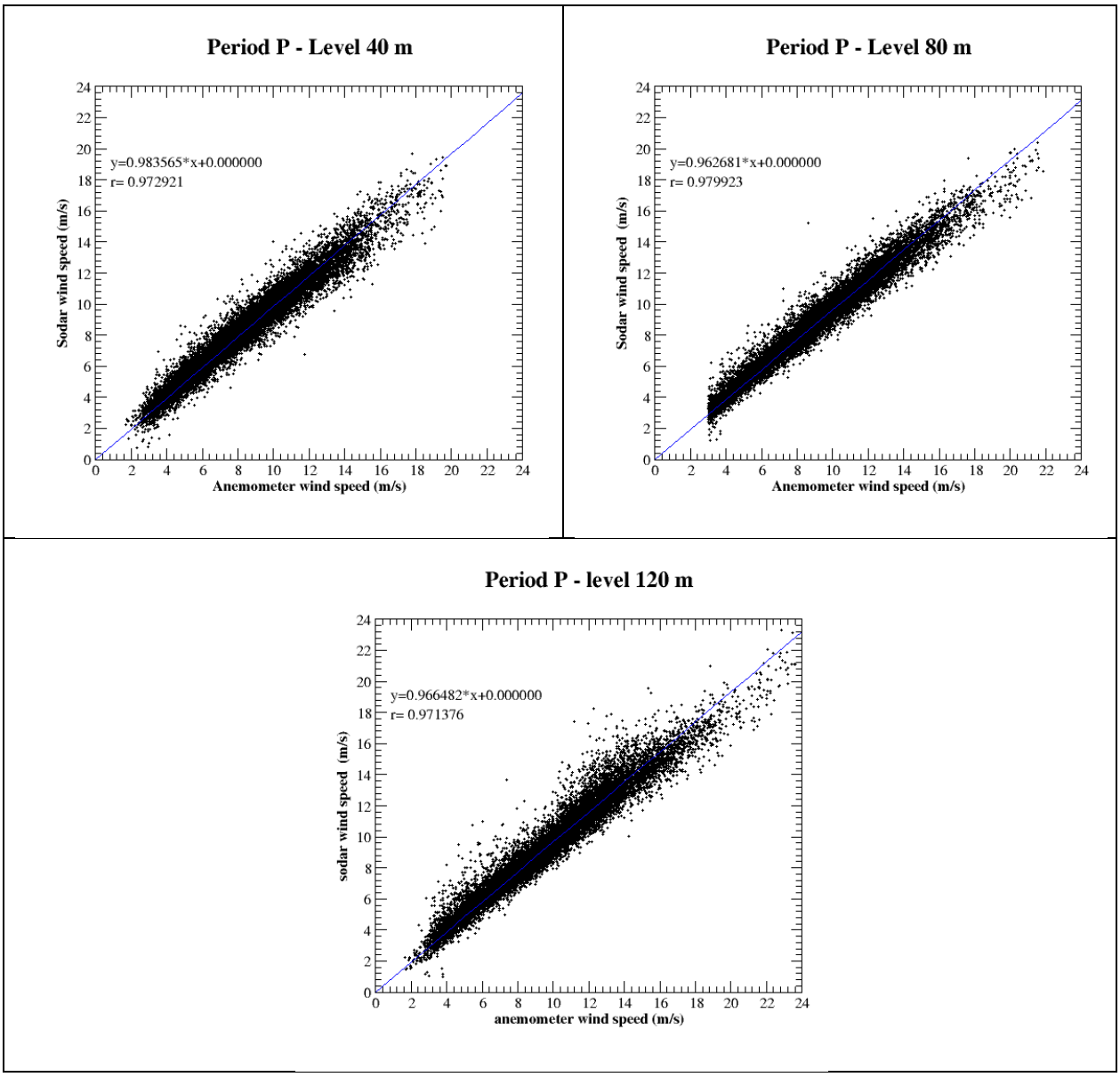

Figure 4-1: Scatter plots of the comparison between Scintec sodar and MP5 mast, at 40m, 80m, and 120m. The offset of the regression line is forced to 0.

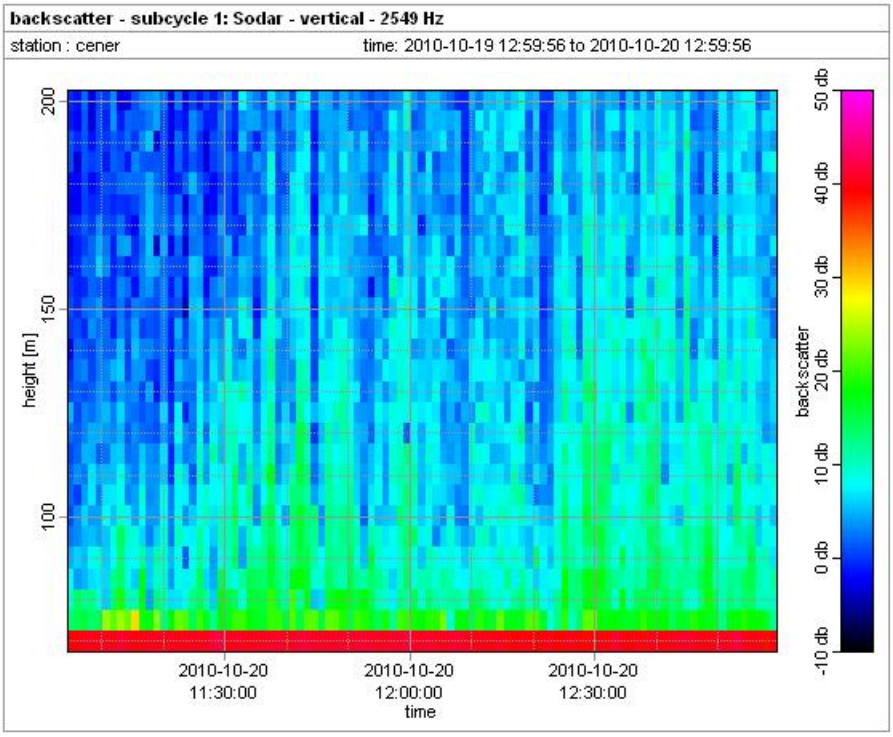

Figure 4-2: Raw data (backscatter) of SFAS sodar for the frequency 2549 Hz and vertical beam, for the 20th of October 2010 between 11 AM and 1 PM.

	40 m	80 m	120 m
bias (m/s)	-0.07	-0.27	-0.24
bias northern winds (m/s)	-0.03	-0.24	-0.08
bias southern winds (m/s)	-0.13	-0.25	-0.32
regression slope	0.984	0.963	0.966
regression slope northern winds	0.991	0.969	0.991
regression slope southern winds	0.977	0.961	0.955
correlation coefficient	0.973	0.980	0.971
correlation coefficient northern winds	0.969	0.976	0.956
correlation coefficient southern winds	0.974	0.978	0.973

Table 4-3 : Statistical scores of the comparison between Scintec sodar and MP5 mast.

5. Comparison between the sodar and the WindCube

The comparison was made separately for the periods P1 (9 215 time samples) and P2 (1 831 time samples), at the same levels as previously: 40 m, 80 m, and 120 m. The scatter plots are shown on figure 5-1, and statistical scores are summarized in table 5-1.

The correlation coefficient is very similar to that observed between the sodar and the mast (between 0.97 and 0.98). A very good agreement between the sodar and the WindCube is observed, with an error close to 0, and a regression slope very close to 1, at 3 height levels. The largest difference (1.4%) is seen during the period P1 for the level 80 m.

Therefore the global wind speed underestimation by the sodar compared to the mast is very similar to the underestimation by the WindCube, which confirms that it is not specific to the sodar but is probably related to the assumption of horizontal homogeneity of the flow, inherent to the remote sensing instruments and which is not valid on complex terrain.

The results obtained during the periods P1 and P2 are very similar. Therefore the differences of the flow characteristics between sodar and MP5 locations are probably weak, which was not obvious initially as the sodar was installed near a modification of the topography on the northern side. However we can note that the difference of 1.4% observed at 80 m during P1 does not appear during P2, and that the correlation coefficient is slightly better during P2 than during P1.

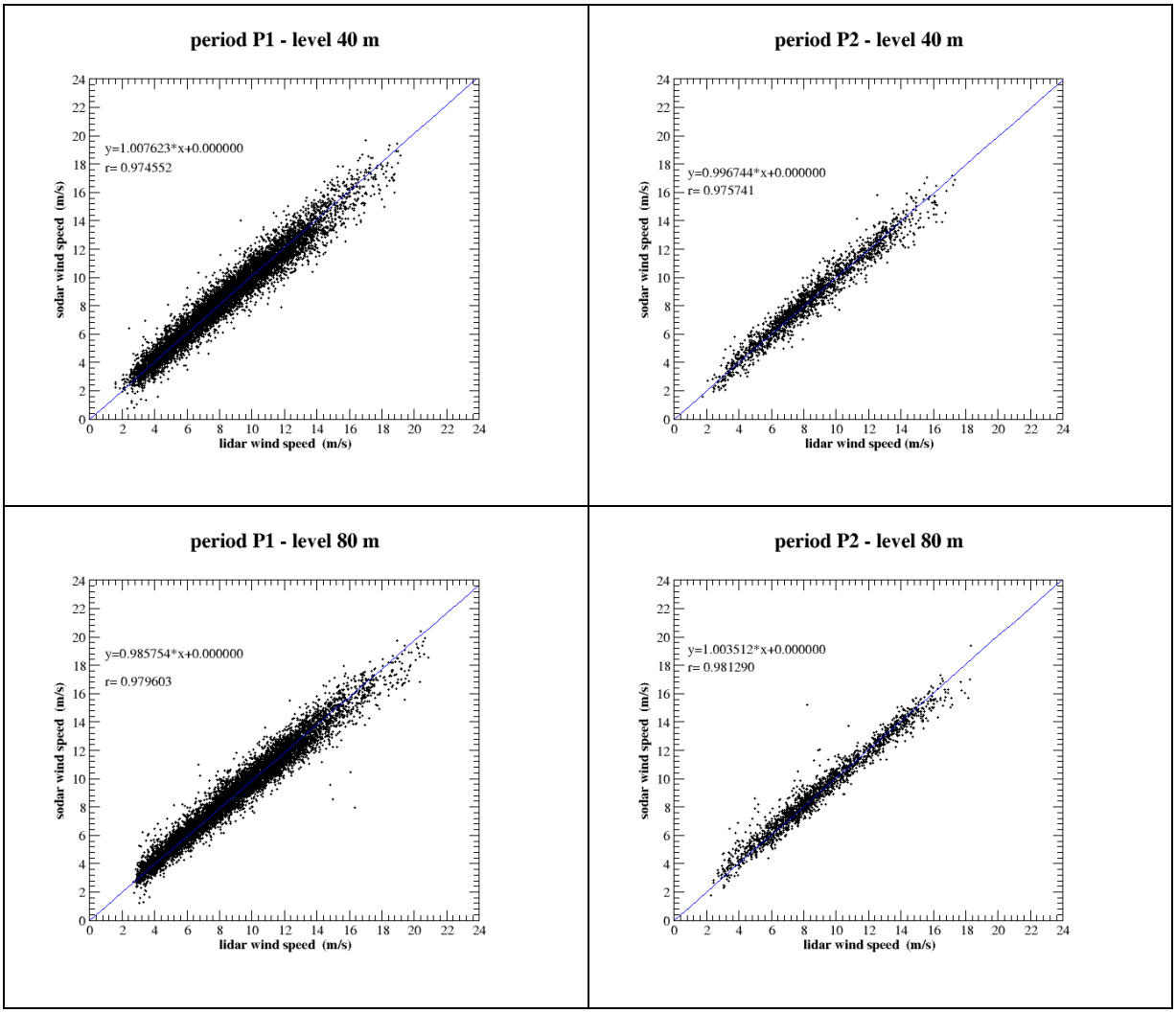

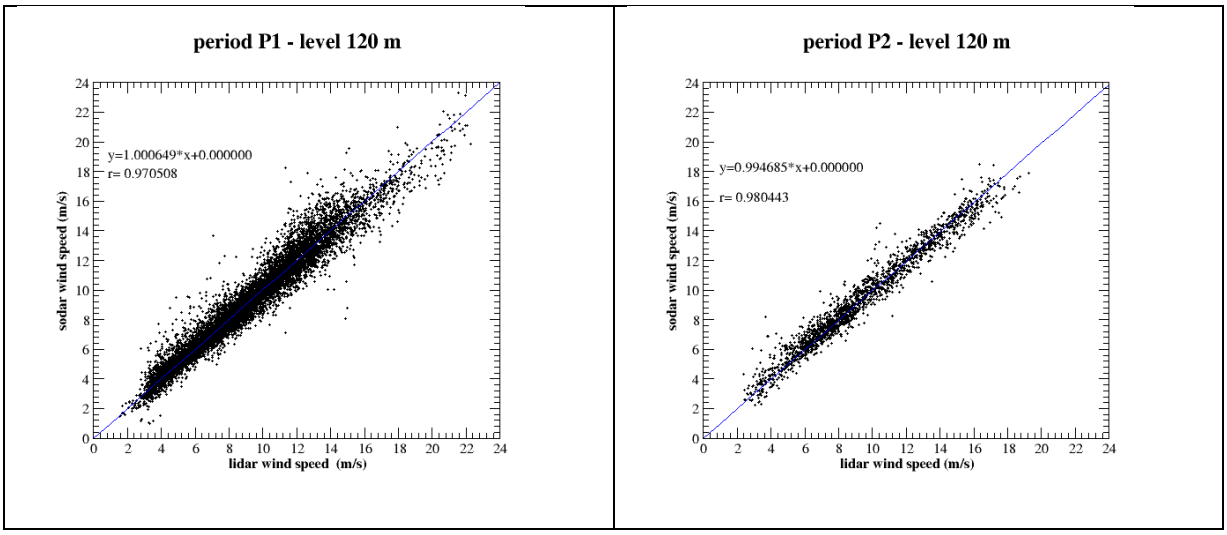

Figure 5-1: Scatter plots of the comparison between SFAS sodar and WindCube, at 40m, 80m, and 120m, during period P1 (left column, SFAS and WindCube not collocated), and during period P2 (right column, SFAS and WindCube collocated). The offset of the regression line is forced to 0.

	40 m	80 m	120 m
bias P1 (m/s)	0.12	-0.07	0.05
bias P2 (m/s)	0.02	0.11	0.03
regression slope P1	1.007	0.986	1.000
regression slope P2	0.997	1.003	0.995
correlation coefficient P1	0.974	0.980	0.971
correlation coefficient P2	0.976	0.981	0.980

Table 5-1: Statistical scores of the comparison between Scintec sodar and WindCube.

6. Summary and Conclusions

6.1 Lidar measurements in complex terrain

The performance of two different lidar systems has been compared to cup anemometer measurements at complex terrain conditions. Identifying the main sources of lidar uncertainty (assuming lidars and cups are properly calibrated) is a difficult task since the studied error sources can affect the measurements simultaneously and identifying their individual contribution is sometimes not possible.

Lidar measurements have been shown to be sensitive to the wind flow uniformity (i.e. spatial wind velocity field variation). The origin of non uniform flows can be due to the orography conditions like the presence of mountains, hills, forests, etc.

It was shown that the variation of the vertical component of the wind velocity plays an important role in the lidar error occurrence for the Alaiz campaign. Tilt angles different from

zero induced the lidars to underestimate the wind speed. It is still necessary to verify if this relationship is causal or if at the lidar siting (mountain edge) the vertical velocity gradient *dw/dx* scales with *w*.

Since lidars work by emitting a laser beam, the presence of low clouds or foggy conditions can be an issue that affects the availability of the device and the quality of the measurements. For the case of the CW lidar used during the measurement campaign, the error due to very low clouds of foggy conditions can reach an order of magnitude greater that the other error sources. The lidar availability was found to be mainly reduced by the presence of low clouds or foggy conditions and less affected by other environmental conditions like rain or snow. Therefore a proper methodology to identify the occurrence of these conditions is very important to assure the quality of the collected data. The CW lidar has been recently upgraded with a new firmware version that is expected to reduce these effects. Yet, more data is necessary to be collected in coming months to assess its effectiveness.

It is important to remember that comparing the lidar data to cup anemometer data, there is always uncertainty in both sensing devices and certain factors can affect their performance either separately or simultaneously. For the cup anemometer, it is of great significance to assess the influence of the met mast where it is installed, the response to the wind flow tilt angle and the effects of icing that can not only stop completely, but also slow down the normal anemometer rotation.

Furthermore, the influence of the atmospheric stability over the wind profile was assessed as well as the lidar capability to measure these effects. It was found that stable atmospheric conditions leads to more pronounced wind shears while neutral and unstable conditions provoke the wind shear to be reduced until becoming almost a vertical line. In general, a negative lidar error increases as the atmosphere becomes more neutrally stratified.

6.2 Sodar measurements in complex terrain

An instrumental inter-comparison has been performed on 10 minutes averaged wind speed between the Scintec SFAS sodar, the Leosphere lidar, and the 120 m high met mast MP5 on Alaiz site. The main conclusions are:

- The correlation coefficient between the SFAS and the mast is about 0.97 to 0.98 at 40m, 80m and 120m. This is consistent with values obtained during previous campaigns performed with this sodar both in flat and complex terrain up to 80 m ([13],[14]), extending this result up to 120 m. The correlation coefficient between the SFAS and the Windcube is also about 0.97 to 0.98.
- The SFAS underestimates wind speed of about 1 to 4 % in comparison with the mast (global error of about -0.1 to -0.3 m/s). This negative error is much lower than during the Høvsøre campaign and is probably not due to ground clutter effect induced by the mast.
- A very good agreement is observed between the SFAS and the Windcube (regression slope very close to 1), which indicates that the negative error of the SFAS is not due to the sodar itself but is probably related to the use of remote sensing instruments in complex terrain without any correction.
- These results have been obtained directly with the data provided by the manufacturer software. Different additional filters have been tested and did not change significantly

the statistical scores, which means that Scintec software is already well optimized for the invalidation of erroneous data.

- The SFAS sodar has shown to be not sensitive to rain, and to be able to measure wind speeds up to more than 22 m/s, with a negative error for wind speeds higher than about 18 m/s.

6.3 Conclusions

From our previous flat terrain campaign, we observed that wind speed measurements obtained with lidar are well correlated to calibrated cup anemometers. In the current campaign at the Alaiz test site, we have seen that complex terrain conditions can introduce an error of up to 10%. This result is similar to that reported by Bingöl et al. (2008) for the Panahaiko site in Greece. Moreover, it was found that the lidar mostly underestimated the mean horizontal wind speed for wind directions coming over the most steep terrain slopes, while the error was closer to zero for wind directions aligned with the flatter region of the hill top. This result is in agreement with the experimental data and theoretical model presented by Bingöl et al. (2008; 2009) and with the theoretical model presented by Bradley (2008).

It is very important to state that although the terrain induced, non-uniform flow introduced a significant error, for the CW lidar tested at Alaiz it was seen that the errors caused by low clouds and fog were much larger. The sensitivity of CW lidars to cloud and fog is already well documented (Smith et al. (2006), Courtney et al. (2008) and Bingöl et al. (2008)). From the experimental results of this campaign it is clear that the CW lidar was unable to measure well in such conditions. However, recent improvements to cloud removal and fog detection algorithms are claimed by the manufacturer.

If a CW is in any case used, it is of high relevance to properly filter out the presence of such conditions. The use of a ceilometer is of great help but this is an additional lidar device that can be costly to acquire. A more sensible solution would be to use a pulsed lidar instead.

The sodar was seen to measure with a similar error to the lidars in respect to the terrain effects. It was not affected by cloud and was able to measure to high wind speeds.

References

[1] Antoniou,I. et al. Remote sensing (UPWIND WP6) six-month progress report. Risø National Laboratory for Sustainable Energy. Roskilde, November 2006

[2] Bingöl, F. et al. LiDAR error estimation with WAsP Engineering. 14th International Symposium for the Advancement of Boundary Layer Remote Sensing. IOP Conf. Series: Earth and Environmental Science 1 (2008) 012058

[3] Bingöl, F. et al. Conically scanning lidar error in complex terrain. Meteorologische Zeitschrift. 2009a; vol. 18, no. 2, p. 189-195

[4] Bingöl, F. et al. Lidar performance in complex terrain modeled by WAsP Engineering. EWEC 2009 Proceedings. Marseille, France, March 2009b

[5] Bingöl, F. et al. Light detection and ranging measurements of wake dynamics. Part I: One-dimensional Scanning. Wind Energy 2010; 13: 51-61

[6] Bouquet, M. et al. Theoretical and CFD analysis of pulsed doppler lidar wind profile measurement process in complex terrain. EWEC 2010 Proceedings. Warsaw, Poland, April 2010

[7] Bradley, S. Wind speed errors for lidars and sodars in complex terrain. 14th International Symposium for the Advancement of Boundary Layer Remote Sensing. IOP Conf. Series: Earth and Environmental Science 1 (2008) 012061

[8] Cabezón, D. et al. RANS simulations of wind flow at the Bolund experiment. EWEC 2010 Proceedings. Warsaw, Poland, April 2010

[9] Clive, P. Compensation of Vector and Volume Averaging Bias in Lidar Wind Speed Measurements. 14th International Symposium for the Advancement of Boundary Layer Remote Sensing. IOP Conf. Series: Earth and Environmental Science 1 (2008) 012036

[10] Conan, B. et al. Feasibility of Micro Siting in Mountainous Terrain by Wind Tunnel Physical Modelling. EWEA 2011 Proceedings. Brussels, March 2011

[11] Courtney, M. et al. Testing and comparison of lidars for profile and turbulence measurements in wind energy. 14th International Symposium for the Advancement of Boundary Layer Remote Sensing. IOP Conf. Series: Earth and Environmental Science 1 (2008) 012021

[12] Dellwik, E. et al. Flow tilt angles near forest edges - Part 2: Lidar anemometry. Biogeosciences, 7, 1759-1768, 2010

[13] Dupont E., J.P. Flori, 2007: Comparison of sodars with ultrasonic and cup anemometers for wind energy applications. European Wind Energy Conference, Milan, 2007

[14] Dupont E., Lefranc Y., Sécolier C., 2009 : A sodar campaign in complex terrain for data quality evaluation and methodological investigations. European Wind Energy Conference, Marseille, 2009

[15] Foussekis, D. et al. Wind profile measurements using a lidar and a 100m mast. EWEC 2007 Proceedings. Milan, Italy, May 2007

[16] Gómez, P. UpWind D6.15.1 Report - An approach to power curve with lidar in complex terrain, 2011

[17] Gomez P., 2011: Measurement campaign in Alaiz – Overview. Deliverable Dc-2.3 of SAFEWIND project.

[18] Gómez, P.et al. Power curve with lidar in complex terrain; Poster. 14th International Symposium for the Advancement of Boundary Layer Remote Sensing. June 2010

[19] Gottschall, J; Courtney, M. Verification test for three WindCube WLS7 lidars at the Høvsøre test site. Report number Risø-R-1732(EN). May 2010

[20] Gottschall, J. et al. Lidar profilers in the context of wind energy – A verification procedure for traceable measurements. Wind Energy (submitted, to be published as Special Issue paper 2011)

[21] Harris, M. et al. Validated adjustment of remote sensing bias in complex terrain using CFD. EWEC 2010 Proceedings. Warsaw, Poland, April 2010

[22] Harris, M. Introduction to continuous-wave Doppler lidar, presentation. Risø PhD Summer School on Remote Sensing. Roskilde, Denmark, June 2010

[23] Hill, C. Remote Sensing (UpWind WP6) QinetiQ Lidar Measurement Report. QinetiQ, Worcs, July 2009a

[24] Hill, C. Remote Sensing (UpWind WP6) QinetiQ Report on Cloud Removal Algorithm. QinetiQ, Worcs, December 2009b

[25] International Standard IEC 61400-12-1. Wind Turbines – Part 12-1: Power performance measurements of electricity producing wind turbines. First edition, 2005

[26] Jaynes, D. et al. Massachusetts Technology Collaborative: Final Progress Report: LIDAR. University of Massachusetts, July, 2007

[27] Lindelöw, P et al. Wind shear proportional errors in the horizontal wind speed sensed by focused, range gated lidars. 14th International Symposium for the Advancement of Boundary Layer Remote Sensing. IOP Conf. Series: Earth and Environmental Science 1 (2008) 012023

[28] Lindelöw, P. UpWind D6.1.3 Report - Uncertainties in wind assessment with lidar. Risø-R-1681(EN). January, 2009

[29] Lindelöw, P et al. Flow distortion on boom mounted cup anemometers. Report number: Risø-R-1738 (E). Risø National Laboratory for Sustainable Energy. Roskilde, July 2010

[30] Mann, J. et al. Lidar Scanning of Momentum Flux in and above the Atmospheric Surface Layer. Journal of atmospheric and oceanic technology, 27, 959–976, 2010

[31] MEASNET - Evaluation of site specific wind conditions. Version 1, November 2009

[32] MEASNET - Anemometer Calibration Procedure. Version 2, October 2009

[33] Mikkelsen, T. Lidar wind speed measurements from a rotating spinner. EWEC 2010 Proceedings. Warsaw, Poland, April 2010

[34] Natural Power - ZephIR laser anemometer brochure.

http://www.naturalpower.com/sites/default/files/file/NaturalPower_ZephIR_Brochure_ecopy.pdf

(last access: [April 2010])

[35] Pedersen, T. et al. ACCUWIND – Classification of five anemometers according to IEC61400-12-1". 2006

[36] Sjöholm, M. et al. Spatial averaging-effects on turbulence measured by a continuous-wave coherent lidar. Meteorologische Zeitschrift, vol. 18, no. 3, p. 281 – 287, June 2009

[37] Smith, D. et al. Wind Lidar Evaluation at the Danish Wind Test Site in Høvsøre. Wind Energy, 9, p. 87–93, January 2006

[38] Stull R.B. An Introduction to Boundary Layer Meteorology, Kluwer Academic Publishers, 1988

[39] Trujillo, J. et al. Arrangements for enhanced measurements of a large turbine near-wake using LiDAR from the nacelle. 14th International Symposium for the Advancement of Boundary Layer Remote Sensing. IOP Conf. Series: Earth and Environmental Science 1 (2008) 012060

[40] UNE-EN ISO/IEC 17025:2000 - Requisitos generales relativos a la competencia de los laboratorios de ensayo y calibración.

[41] Wagner, R et al. Investigation on turbulence measurements with continuous wave, conically scanning LiDAR. Report number Risø-R-1682(EN). March 2009a

[42] Wagner, R et al. MultiMW wind turbine power curve measurement using a lidar (second Høvsøre campaign). Report number Risø-I-2954(EN). September 2009b

[43] Wagner, R. Accounting for the speed shear in wind turbine power performance measurement. Risø-PhD-58(EN) - Short version. Risø National Laboratory for Sustainable Energy. Roskilde, April 2010

[44] WindScanner project homepage.

http://www.risoe.dtu.dk/research/sustainable_energy/wind_energy/projects/vea_wind_scanner.aspx?sc_lang=en/

[last access: October 2011]